Cytometry PART A
ISAC
Journal of Quantitative Cell Science

MIFlowCyt

OMIP-054: Broad Immune Phenotyping of Innate and Adaptive Leukocytes in the Brain, Spleen, and Bone Marrow of an Orthotopic Murine Glioblastoma Model by Mass Cytometry

Sophie A. Dusoswa, Jan Verhoeff, Juan J. Garcia-Vallejo*

Amsterdam UMC, Vrije Universiteit Amsterdam, Department of Molecular Cell Biology & Immunology, Amsterdam Infection & Immunity Institute and Cancer Center Amsterdam, Amsterdam, The Netherlands

Received 2 August 2018; Revised 10 January 2019; Accepted 14 January 2019

Grant sponsor: Cancer Center Amsterdam, the Netherlands; Grant sponsor: Institute Chemical Immunology, the Netherlands

Additional Supporting Information may be found in the online version of this article.

*Correspondence to: Dr. Juan J. Garcia Vallejo, Amsterdam UMC, Vrije Universiteit Amsterdam, Department of Molecular Cell Biology & Immunology, Amsterdam Infection & Immunity Institute and Cancer Center Amsterdam, de Boelelaan 1108, Amsterdam 1081 HZ, The Netherlands.
Email: jj.garciavallejo@vumc.nl

Published online 31 January 2019 in Wiley Online Library (wileyonlinelibrary.com)

DOI: 10.1002/cyto.a.23725

ISAC
International Society for Advancement of Cytometry

Purpose and Appropriate Sample Types

Here we present a 42 parameter panel to characterize myeloid immune cell subsets and T lymphocyte activation status in cryopreserved and barcoded single cell suspensions obtained from brain, spleen, and bone marrow of an orthotopic immunocompetent glioblastoma mouse model in a C57BL/6 background (Table 1). This panel is designed for mass cytometry by time of flight (CyTOF) and combines 34 antibodies against diverse cell surface and intracellular targets together with cisplatin for live/dead discrimination, iridium for cell identification, and six cellular barcodes (1) to enable simultaneous multiplexed acquisition of up to 20 samples (Table 2). The panel is designed for a comprehensive evaluation of the immune system in different organs during murine in vivo studies in the field of glioblastoma immunology, but could also be applied to other disease models in the central nervous system (CNS) with possible systemic involvement, such as brain metastasis arising from other types of cancer, experimental autoimmune encephalomyelitis (EAE), or neurodegenerative disease models. Marker selection was partly based on a combination of previously reported panels studying CNS immune infiltrates (2–7). The selected set of markers captures T lymphocytes (CD8+, CD4+, and regulatory T lymphocytes), dendritic cells (DC), monocytes, macrophages, microglia, tumor cells (when GFP positive), and granulocytes, and contains a set of antibodies to detect cell activation, migratory capacity and immune checkpoints (Table 2). The panel has been optimized with respect to marker selection, antibody clone usage, antibody-metal pairing, and antibody concentration, and has room for additional markers by filling in a number of free channels as listed in Table 2.

Background

In the last decades enormous efforts have been made to develop therapeutic interventions that boost antitumor immunity, including adoptive cell transfer, anticancer vaccination, application of oncolytic viruses, and immune checkpoint inhibition (8,9). A wide range of immunotherapeutic strategies are being tested in glioblastoma, advanced by successes in other tumor types. In these approaches particularly T cells are targeted as final effector cells by, for example, dendritic cell vaccination or immune checkpoint inhibition, but durable responses remain limited to case reports (10). Boosted T cell responses as a result of, for example, vaccination strategies encounter functional impairment due to immune inhibitory mechanisms both in the tumor microenvironment and systemically. To overcome T cell inhibition hope was pinned on immune checkpoint inhibition with monoclonal antibody therapy against PD1 and CTLA-4. Nevertheless, to date clinical trials testing immune

Table 1. Summary table for the application of this OMIP

PURPOSE	IMMUNOPHENOTYPING OF INNATE AND ADAPTIVE IMMUNE CELLS IN A MURINE GLIOBLASTOMA MODEL
Species	Mouse
Cell types	Single cells from Miltenyi neural tissue dissociation kit (P) treated brain
Cross-references	No similar OMIP

checkpoint inhibition in glioblastoma have not shown impressive results (11). Clearly glioblastoma-specific immune suppression is a complex and unsolved problem that remains an obstacle for successful immunotherapies. Therefore, a better understanding of glioblastoma immune escape and contributing factors is warranted, alongside the development of biomarkers for patient selection and prediction of clinical response. Immune suppression in glioblastoma is largely mediated by infiltration of monocytes into the glioblastoma microenvironment (12). Myeloid immune cells dominate immune infiltrates and are involved in glioblastoma disease progression (13–15). Although some subsets have been studied in isolation, the different types of infiltrating myeloid and lymphoid cells, their recruitment from the bone marrow and spleen, and their phenotypic distribution need further investigation.

Mass cytometry provides for the simultaneous measurement of more than 40 parameters at single cell resolution, improving the ability of cytometry to characterize the complexity of the immune system (16). Similar to the development of antibody panels for multichromatic fluorescence cytometry, mass cytometry panel development requires optimization of antibody-metal pairing, conjugation of antibodies with metal polymers, determination of optimal antibody concentrations, and optimization of buffers and staining conditions. Here we developed a mass cytometry immunophenotyping panel, which was designed to quantify population frequencies and to infer functional states of T cells, including activation, differentiation, exhaustion, or anergy in the murine glioblastoma microenvironment (Fig. 1) and spleen. Furthermore, our panel helps to differentiate and quantify a multitude of glioblastoma infiltrating and bone marrow derived myeloid cell subsets and immune cells resident to the bone marrow. Although this panel is optimized for single cell suspensions obtained from mouse brain, spleen, and bone marrow it could also be applied to the study of innate and adaptive components of the immune system in other mouse organs. Single cell suspensions were generated using mechanical dissociation and enzymatic digestion using the Neural Tissue Dissociation kit P (Miltenyi, Germany) (17). After live/dead staining and barcoding (1) cells were cryopreserved until antibody staining and mass cytometry analysis (Fig. 1A). Following data pre-processing including bead normalization (18) and debarcoding (1), the first gates aimed at exclusion of normalization beads, cell debris, doublets, and dead cells ($^{140}Ce^{-}$, $^{193}Ir^{+}$, and $^{194}Pt^{-}$). Next, we plotted CD45 against CD11c to identify $CD45^{hi}CD11c^{hi}$ DCs (population 1). Plotting CD45 against CD11b for non-DCs resulted in four main populations: $CD45^{-}$ non-immune cells (population 2), $CD45^{+}CD11b^{-}$ lymphocytes, $CD45^{+}CD11b^{+}$ infiltrating myeloid cells, and $CD45^{dim}CD11b^{+}$ microglia. $CD45^{-}$ cells include tumor cells and non-immune non-tumor brain resident cells, such as glial cells or neurons. In the $CD45^{+}CD11b^{-}CD3^{+}TCRb^{+}$ cells we identified $CD8^{+}$ T cells, $CD4^{+}$ T cells, and $CD4^{+}FoxP3^{+}$ regulatory T cells (populations 3, 4, and 5, respectively). Next, we identified microglia as being the $CD44^{-}CD49d^{-}$ cells in the $CD11b^{+}CD45^{dim}$ population (population 6). Based on MHC-II, CCR2, and PD-L1 expression we identified three clusters of microglia with different activation states (6A, 6B, 6C). $CD45^{+}CD11b^{+}$ infiltrating myeloid cells contain granulocytes (population 7), $Ly6C^{hi}CCR2^{hi}$ recently extravasated monocytes (population 8), and some clusters of macrophages with different phenotypes and/or states of activation (9A, 9B, 9C, 9D, 9E, and 9F) based on their expression of CCR2, MHC-II, PD-L1, CD38, and CD88. Gated populations were identified based on two-dimensional embeddings of the high dimensional space visualized using the viSNE algorithm in Cytobank (Fig. 1B,C).

Enzymatic digestions often result in the cleavage of molecules on the membrane of immune cells, which could have detrimental effect in their recognition by antibodies. In order to allow direct comparison amongst different organs (brain, spleen, and bone marrow) all samples were subjected to the same enzymatic treatment as it was required for the processing of the brain samples. The panel presented in this OMIP has been optimized to the single cell suspension preparation procedure as suggested by the manufacturer with some minor adjustments (see Supporting Information "Online Protocol"). Care should be taken to specifically address any effects of alterations in the tissue dissociation protocol to the performance of this panel.

Similarity to Other OMIPs

This OMIP is partly overlapping with OMIP-032, which describes two murine multicolor immunofluorescence panels including the following markers to detect B and T lymphocytes, natural killer cells, dendritic cells, macrophages, monocytes, and neutrophils: CD45, TCRβ, CD4, CD8, Ly6C, CD49b, Ly6G, CD11c, MHCII, CD206, NKp46, CD62L, and CD44 (19). These markers overlap with our panel except for CD49b, NKp46, and CD62L. Since our panel is more focused on activation and exhaustion in T lymphocytes, we included more antibodies against activation markers and co-inhibitory molecules (immune checkpoints) rather than the presence of naïve or memory T cells. Also OMIP-031 has overlap with a panel aimed at immune checkpoint expression (20), which reports the following markers: CD3, CD4, CD8, CD69, CD44, CD45RA, CD27, CD62L, KLRG127, CD127, PD-1, CTLA4, TIM-3, LAG-3, and CD45. Our panel includes all of these markers except for CD45RA, CD27, CD62L, KLG127, and LAG-3. Previously, three other mass cytometry panels have been published. They focus on the characterization of human peripheral leukocytes (OMIP-34), human head and neck

Table 2. Summary table for the antibodies in this panel

TARGET PROTEIN	CLONE	METAL	SOURCE	PURPOSE
Cell identification				
Barcodes		103–110Pd	Fluidigm	Staining standardization and doublet discrimination
Iridium		191–193Ir	Fluidigm	Cell identification
Cisplatin		194–195Pt	Fluidigm	Live/dead discrimination
Cell classification				
CD45	30-F11	89Y	Fluidigm	All leukocytes
CD3e	145-2C11	152Sm	Fluidigm	T lymphocytes
TCRb	H57-597	169Tm	Fluidigm	T a/b lymphocyte receptor
CD4	RM4-5	145Nd	Fluidigm	T helper lymphocytes
Foxp3 (FJK16s)	FJK-16s	158Gd	Fluidigm	Regulatory T lymphocytes
CD8b	536.7	168Er	Fluidigm	Cytotoxic T lymphocytes
CD127 (IL-7Ra)	A7R34	175Lu	Fluidigm	Memory T lymphocytes
CD28	37.51	151Eu	Fluidigm	T lymphocytes, natural killer cells
Ly-6G	1A8	141Pr	Fluidigm	Granulocytes
Ly-6C	HK1.4	150Nd	Fluidigm	Monocytes, macrophages
CD11b (Mac-1)	M1/70	148Nd	Fluidigm	Macrophages, microglia, dendritic cells, granulocytes
CD11c	N418	209Bi	Fluidigm	Dendritic cells
CD14	Sa14-2	144Nd	Biolegend	Monocytes
CD88	20/70	161Dy	Biolegend	Monocytes, macrophages, neutrophils, eosinophils
MHC class 2 I-A/I-E	M5/114.15.2	174Yb	Fluidigm	Antigen presenting cells, T lymphocyte activation?
TMEM119	106–6	146Nd	Abcam	Microglia
CD49d	R1-2	176Yb	Biolegend	Exclusion marker for microglia
CD169 (Siglec-1)	3D6.112	142Nd	Biolegend	Dendritic cells, macrophages, microglia
CD206 (Mannose receptor)	C068C2	160Gd	Biolegend	Macrophages, dendritic cells
Siglec H	440c	166Er	Genetex	Plasmacytoid dendritic cells, Microglia
CD38	90	153Eu	Biolegend	B lymphocyte (pre-cursors), macrophages
aGFP	454,505	173Yb	Biolegend	Tumor cells
Migration				
CCR2	475,301	165Ho	RnD systems	Monocyte chemotaxis
CCR6	29-2L17	156Gd	Fluidigm	Dendritic cell- and lymphocyte chemotaxis
CD54 (ICAM-1)	YN1/1.7.4	163Dy	Fluidigm	Leukocyte extravasation
Activation				
Ly-6A/E (Sca-1)	D7	164Dy	Fluidigm	Hematopoietic stem cell marker/ activation of lymphocytes
Ki-67	B56	172Yb	Fluidigm	Cell proliferation
CD69	H1.2F3	143Nd	Fluidigm	Activated T lymphocytes
CD44	IM7	171Yb	Fluidigm	Activated lymphocytes
CD150 (SLAM, IPO-3)	TC15-12F12.2	167Er	Fluidigm	Activated lymphocytes and dendritic cells
Immune checkpoints				
CD152 (CTLA-4)	UC10-4B9	154Sm	Fluidigm	Co-inhibitory molecule
CD279 (PD-1)	J43	159Tb	Fluidigm	Co-inhibitory molecule
CD274 (PD-L1)	10F.9G2	155Gd	Biolegend	PD1 ligand
CD366 (Tim-3)	RMT3-23	162Dy	Fluidigm	Co-inhibitory molecule
Free channels				
		113–115In		
		147Sm		
		149Sm		
		170Er		

cancer (OMIP-45), and the quantification of calcium sensors and channels in lymphocyte subsets (21–23). This is the first mass cytometry OMIP for a comprehensive characterization of the mouse immune system. All data used generated during the optimization and verification of this panel can be found in FlowRepository under ID: FR-FCM-ZYUF.

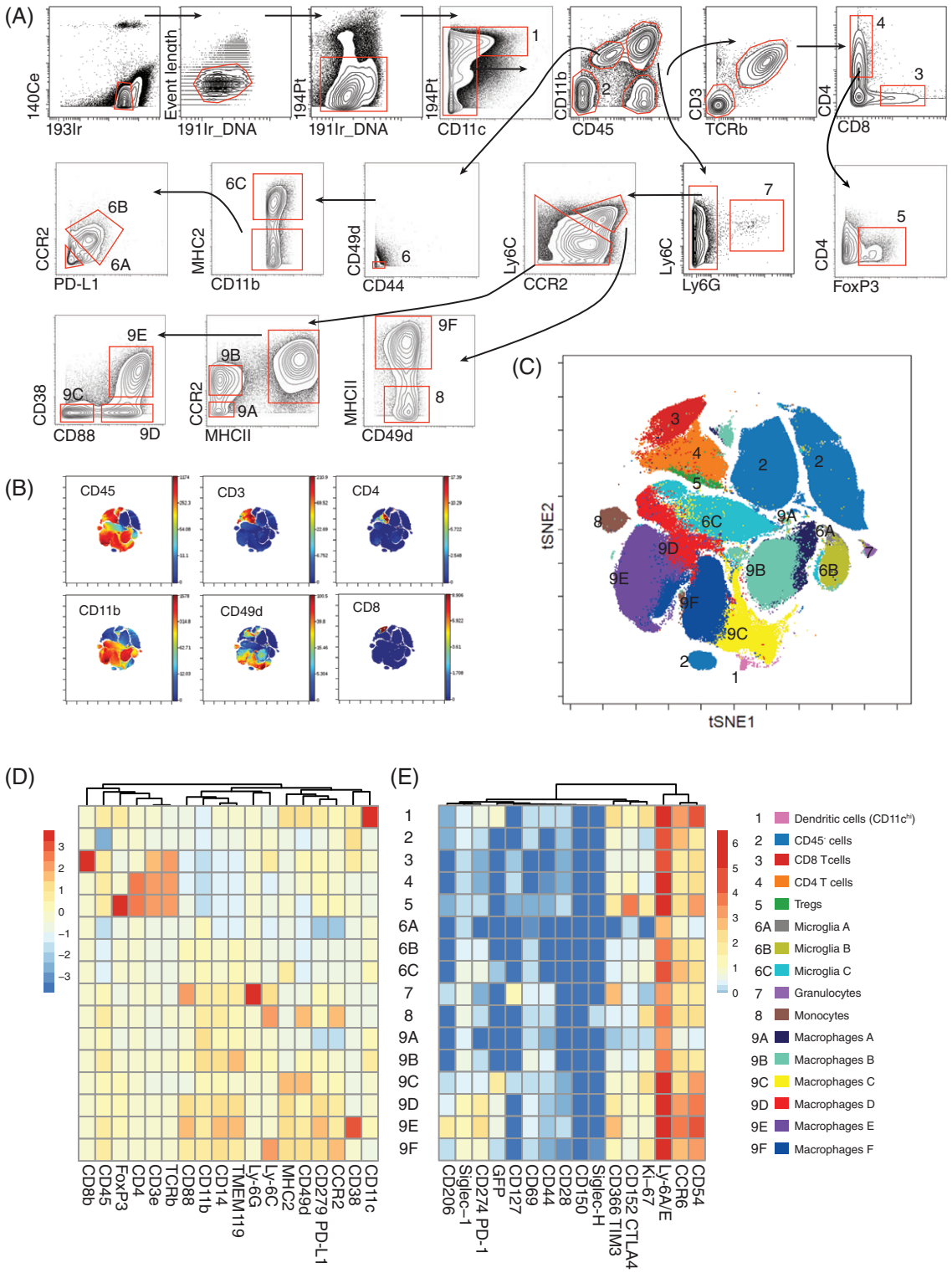

Figure 1. Identification of main leukocyte populations and CD45^{-} cells in murine glioblastoma by manual gating and representation by viSNE. (**A**) Example gating of cell subsets. (**B**) viSNE embeddings color-coded for lineage markers. (**C**) Populations gated in A are color-coded according to the legend inset and displayed in the viSNE map. (**D**) Heatmap describing relative expression of lineage markers across the populations described in A, B, and C. (**E**) Heatmap displaying median mass intensity (ArcSinH(5)-transformed) of activation and migration markers across the populations described in A, B, and C. [Color figure can be viewed at wileyonlinelibrary.com]

Acknowledgments

We thank Prof. van Kooyk (Amsterdam UMC, Location VUmc) for fruitful discussions and laboratory resources. We also thank S. Schetters, Dr. Crommentuijn (both from Amsterdam UMC, Location VUmc), E. Abels (Massachusetts General Hospital), and Dr. Broekman (Leiden University Medical Center) for discussions and suggestions during panel design. We thank E. Abels for providing samples for optimization experiments.

Author Contributions

SAD and JV performed experiments. SAD and JV developed and optimized the panel. SAD, JV, and JJGV discussed panel design and optimization. SAD and JJGV wrote the article. The authors declare that they have no conflict of interest.

Literature Cited

1. Zunder ER, Finck R, Behbehani GK, Amir EAD, Krishnaswamy S, Gonzalez VD, Lorang CG, Bjornson Z, Spitzer MH, Bodenmiller B, et al. Palladium-based mass tag cell barcoding with a doublet-filtering scheme and single-cell deconvolution algorithm. Nat Protoc 2015;10:316–333.
2. Korin B, Ben-Shaanan TL, Schiller M, Dubovik T, Azulay-Debby H, Boshnak NT, Koren T, Rolls A. High-dimensional, single-cell characterization of the brain's immune compartment. Nat Neurosci 2017;20:1300–1309. https://doi.org/10.1038/nn.4610.
3. Ajami B, Samusik N, Wieghofer P, Ho PP, Crotti A, Bjornson Z, Prinz M, Fantl WJ, Nolan GP, Steinman L. Single-cell mass cytometry reveals distinct populations of brain myeloid cells in mouse neuroinflammation and neurodegeneration models. Nat Neurosci 2018;21:541–551. https://doi.org/10.1038/s41593-018-0100-x.
4. Mrdjen D, Pavlovic A, Hartmann FJ, Schreiner B, et al. High-dimensional single-cell mapping of central nervous system immune cells reveals distinct myeloid subsets in health, aging, and disease. Immunity 2018;48:380–395.
5. Bowman RL, Klemm F, Akkari L, Pyonteck SM, Sevenich L, Quail DF, Dhara S, Simpson K, Gardner EE, Iacobuzio-Donahue CA, et al. Macrophage ontogeny underlies differences in tumor-specific education in brain malignancies. Cell Rep 2016;17:2445–2459.
6. Chen Z, Feng X, Herting CJ, Garcia VA, Nie K, Pong WW, Rasmussen R, Dwivedi B, Seby S, Wolf SA, et al. Cellular and molecular identity of tumor-associated macrophages in glioblastoma. Cancer Res 2017;77:2266–2278.
7. Bennett ML, Bennett FC, Liddelow SA, Ajami B, Zamanian JL, Fernhoff NB, Mulinyawe SB, Bohlen CJ, Adil A, Tucker A, et al. New tools for studying microglia in the mouse and human CNS. Proc Natl Acad Sci U S A 2016;113:E1738–E1746.
8. Chen DS, Mellman I. Oncology meets immunology: The cancer-immunity cycle. Immunity 2013;39:1–10.
9. Galluzzi L, Vacchelli E, Bravo-San Pedro JM, et al. Classification of current anticancer immunotherapies. Oncotarget 2014;5:12472–12508.
10. Lim M, Xia Y, Bettegowda C, Weller M. Current state of immunotherapy for glioblastoma. Nat Rev Clin Oncol 2018;15:422–442. https://doi.org/10.1038/s41571-018-0003-5.
11. Maxwell R, Jackson CM, Lim M. Clinical trials investigating immune checkpoint blockade in Glioblastoma. Curr Treat Options Oncol 2017;18:51.
12. Wurdinger T, Deumelandt K, van der Vliet HJ, Wesseling P, de Gruijl TD. Mechanisms of intimate and long-distance cross-talk between glioma and myeloid cells: How to break a vicious cycle. Biochim Biophys Acta Rev Cancer 2014;1846:560–575.
13. Broekman ML, Maas SLN, Abels ER, Mempel TR, Krichevsky AM, Breakefield XO. Multidimensional communication in the microenvirons of glioblastoma. Nat Rev Neurol 2018;14:482–495. https://doi.org/10.1038/s41582-018-0025-8.
14. Quail DF, Joyce JA. The microenvironmental landscape of brain tumors. Cancer Cell 2017;31:326–341.
15. Hambardzumyan D, Gutmann DH, Kettenmann H. The role of microglia and macrophages in glioma maintenance and progression. Nat Neurosci 2015;19:20–27.
16. Spitzer MH, Nolan GP. Mass cytometry: Single cells, many features. Cell 2016;165:780–791.
17. Hussain RZ, Miller-Little WA, Doelger R, Cutter GR, Loof N, Cravens PD, Stüve O. Defining standard enzymatic dissociation methods for individual brains and spinal cords in EAE. Neurol Neuroimmunol NeuroInflamm 2018;5:1–10.
18. Finck R, Simonds EF, Jager A, Krishnaswamy S, Sachs K, Fantl W, Pe'er D, Nolan GP, Bendall SC. Normalization of mass cytometry data with bead standards. Cytometry Part A 2013;83A:483–494.
19. Unsworth A, Anderson R, Haynes N, Britt K. OMIP-032: Two multi-color immunophenotyping panels for assessing the innate and adaptive immune cells in the mouse mammary gland. Cytometry Part A 2016;89A:527–530.
20. Nemoto S, Mailloux AW, Kroeger J, Mulé JJ. OMIP-031: Immunologic checkpoint expression on murine effector and memory T-cell subsets. Cytometry Part A 2016;89A:427–429.
21. Baumgart S, Peddinghaus A, Schulte-Wrede U, Mei HE, Grützkau A. OMIP-034: Comprehensive immune phenotyping of human peripheral leukocytes by mass cytometry for monitoring immunomodulatory therapies. Cytometry Part A 2017;91A:34–38.
22. Brodie TM, Tosevski V, Medová M. OMIP-045: Characterizing human head and neck tumors and cancer cell lines with mass cytometry. Cytometry Part A 2018;93A:406–410.
23. Jaracz-Ros A, Hémon P, Krzysiek R, Bachelerie F, Schlecht-Louf G, Gary-Gouy H. OMIP-048 MC: Quantification of calcium sensors and channels expression in lymphocyte subsets by mass cytometry. Cytometry A 2018;93:681–684.